Orissa Journal of Physics
ISSN 0974-8202

Vol. 24, No.1
February 2017
pp. 133-141

Complex Impedance and Conductivity Studies of Nd Doped Ferroelectric Oxide

S BEHERA[1], P R DAS[2]* and P NAYAK[3]

[1]Department of Physics, School of Applied Science, CUTM, Bhubaneswar-752050, India
[2]Department of Physics, VSSUTechnology, Burla-768018, India
[3]School of Physics, Sambalpur University, Burla - 768019, India
E-mail: prdas63@gmail.com, prdas_phy@vssut.ac.in

Received: 27.11.2016 ; *Revised : 10.12.2016* ; *Accepted : 10.1.2017*

Abstract. In the present work, electrical properties of tungsten-bronze structured $Na_2Pb_2Nd_2W_2Ti_4Ta_4O_{30}$ ceramic, synthesized by conventional high temperature solid-state reaction route, have been studied using complex impedance spectroscopy. Compound formation and phase identification has been confirmed by X-ray diffraction (XRD). Impedance (experimental and theoretical fitting), modulus and electrical conductivity of the material exhibit a strong correlation between its micro-structure (i.e., bulk, grain boundary, etc) and electrical parameters. The nature of temperature variation of dc conductivity follows Arrhenius rules. The frequency dependence ac conductivity (fitting) shows the signature of Jonscher's universal power law. The existence of non-exponential-type of conductivity relaxation in the compound was confirmed by detailed studies of its transport properties. It shows that the material has negative temperature co-efficient of resistance similar to that of semiconductors. The same behavior has also been observed in the study of I–V characteristics of the material.

Keywords: Ferroelectricity, Electrical Conductivity, Electrical Impedance,

PACS No: 77.80.-e, 72.80.Tm, 87.63.Pn

1. Introduction

Among all the ferroelectric compounds known today, some oxides of tungsten bronze (TB) structural families have been found very fascinating for piezoelectric, pyro electric, microwave dielectric/resonators, etc. devices at room temperature [1-3] because of their high device parameters. The TB structure has arrays of distorted BO_6 octahedral sharing corners in such a way that three different types of interstices (A, B and C) can be utilized for designing and developing a large number of new compounds of a general formula $[(A_1)_2(A_2)_2(A_3)_2(C)_4][(B_1)_2(B_2)_4(B_3)_4]O_{30}$. As the smallest interstice C is generally

empty or the smallest, the filled tungsten bronze structure could have a general formula $A_6B_{10}O_{30}$. Because of the complex crystal structure, the properties of tungsten bronze structure could be modified further in a wide to make it interesting and useful for devices. After being the first research group to report ferroelectric properties in compounds having mono divalent and rare earth ions substituted at the A site, and tetra-hexavalent ions substituted at the B site [4-9], we continue our endeavor for search of new compounds for device applications. In the process we have reported synthesis, structural, microstructure and dielectric properties of titled compound [10]. In this paper we have extended our work by investigating the electrical properties using impedance spectroscopy technique for the titled material.

2. Experimental

The Polycrystalline sample of $Na_2Pb_2Nd_2W_2Ti_4Ta_4O_{30}$ (abbreviated as NPNWTT) was prepared by solid state reaction technique using high purity ingredients Na_2CO_3, PbO, Nd_2O_3, WO_3, TiO_2, and Ta_2O_5. These ingredients taken in suitable stoichiometry were thoroughly mixed and ground in dry and wet (methanol) medium for 1 h each in an agate mortar. Calcination was carried out in an alumina crucible at 1175^0C for 6 h. The quality and formation of the compound were checked using X-ray diffractometer ((RigakuMiniflex, Cukα, λ = 1.5405Å) over a wide range of Bragg angles 2θ ($20^0 \leq 2\theta \leq 80°$). The powder was then pelletized under the uniaxial pressure of 3.5 ton with polyvinyl alcohol (PVA) as binder. The pellets were then sintered at 1200 ^{0}C for 6 h. The sintered pellets were polished and electrode with silver paste and then dried at 150 ^{0}C for 1 h. The dielectric and impedance parameters of the pellet were recorded as a function of frequency (1 kHz to 1 MHz) using a computer-controlled HIOKI 3532 LCR Hitester over a wide range of temperature.

3. Results and discussion

3.1 Complex Impedance Analysis

The dielectric properties of ferroelectric materials arise due to intra-grain, inter-grain and other electrode effects. The high insulating properties in the dielectric material are caused mainly by the grain boundaries acting as high resistive barriers for cross-transport of charge carriers. Therefore a proper understandingof the effects of grain boundaries is required to evaluate the overall behavior of the ceramic samples.Complex impedance spectroscopy (CIS) technique [11] has been recognized as a powerful non-destructive technique to

study the microstructure and electrical properties of polycrystalline sample. Thus the dynamics of ionic movement and the contributions of various micro structural elements such as grains, grain boundaries and interface polarization to the total dielectric response in polycrystalline solids can be identified by this technique. Measurements of impedance and related parameters of the materials provide us some important data having both real (resistive) and imaginary (reactive) components. These components are calculated using some basic equations: complex impedance$Z(\omega) = Z' - jZ'' = R_s - \frac{j}{\omega C_s}$, complex electrical modulus$M(\omega) = \frac{1}{\varepsilon(\omega)} = M' + j\,M'' = j\,\omega CoZ$, complex admittance $Y^* = Y' + jY'' = j\omega C_o\varepsilon^* = (R_P)^{-1} + j\omega C_p$ and complex permittivity $\varepsilon^* = \varepsilon' - j\varepsilon''$where $\omega = 2\pi f$ is the angular frequency; C_0 is the geometrical capacitance, $j = \sqrt{-1}$and subscripts p and s are parallel and series circuit components respectively.

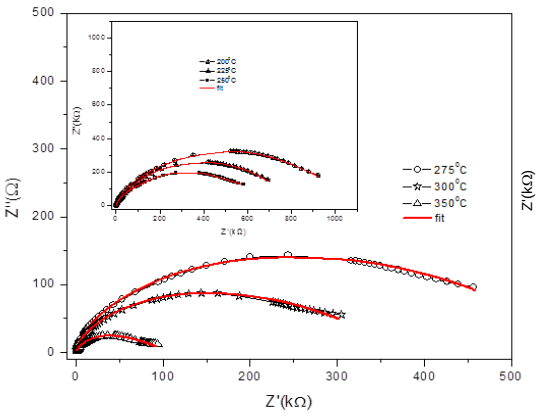

Fig.1. Variation of Z″ with Z′ of NNdT at different temperatures.

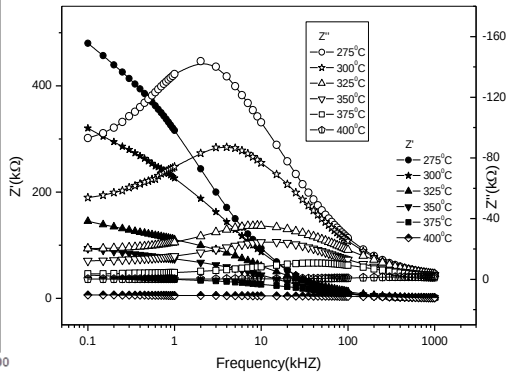

Fig.2. Variation of Z′ and Z″ with frequency of NNdT at different temperatures.

Figure 1.shows the complex impedance spectra (Nyquist plot) with fitted data [12] of the compound obtained at different temperatures (>300^{0}C) over a wide frequencyrange (1 KHz to 1 MHz). The linear response in Z″ (not shown here) at lower temperature (≤250^{0}C) indicates the insulating behavior in the sample. As the temperature increases above 350^{0}C the linear response gradually change to semicircles which became smaller and shifts towards lower Z′ values, indicating a reduction in grain (R_g) and grain boundary (R_{gb}) resistance [13].The presence of the semicircular arcs for temperatures up to 350^{0}C suggests that the electrical processes in the material arises basically due to the contribution from

bulk material (grain interior), which can thus be modeled as an equivalent electrical circuit comprising a parallel combination of a bulk resistance (R_b) and bulk capacitance (C_b) [14].The emergence of a second semicircular arc for temperatures above 375^0C confirms the additional contribution from grain boundary. For ideal Debye-type relaxation, a perfect semicircle with its center on the Z′-axis should be observed. All the semicircles exhibit some depression instead of a semicircle centered on the Z′-axis. Such behavior is indicative of non-Debye type of relaxation and it also manifests that there is a distribution of relaxation time instead of a single relaxation time in the material [15].The value of bulk resistance (R_b) at different temperatures has been obtained from the intercept of the semicircular arcs on the real axis (*Z′).*

Fig.2. shows the variation of Z′ and Z″ as a function of frequency at some selected temperatures. The value of Z′ decreases with rise in frequency and temperature which is related to the electrical conductivity of the material. At high frequency the value of Z′ at each temperature coincides implying the possible release of space charge [16].

At different temperatures, it is observed that with increase in frequency the value of Z″ increases to a maximum (Z''_{max}) and then decreases. This explains the presence of relaxation in the sample. The broadening of Z''_{max} peak with increase of temperature is a clear indication of the occurrence of temperature dependence of relaxation phenomenon in the material. The relaxation process occurs due to the presence of immobile charges at low temperatures and inherent defects and vacancies created during higher temperature processing of the sample [17, 18].

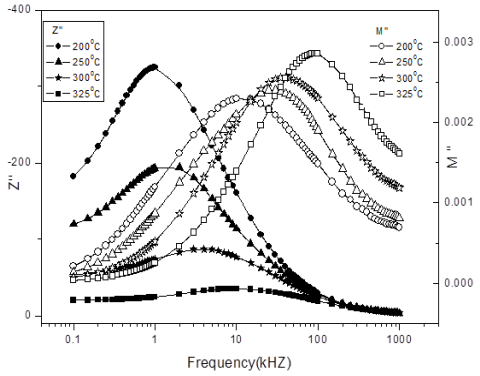

Fig.3. Variation of M" and Z" with frequency at different temperatures of NNdT.

The imaginary components of impedance (Z″) and modulus (M″) are plotted with frequency (Fig. 3) at selected temperatures to detect the presence of the smallest capacitance and the largest resistance [19]. This plot also helps to

distinguish whether relaxation process is due to short range or long range motion of charge carriers. For the short range process, peaks of Z″ and M″ will occur at different frequencies whereas for long range they will occur at same frequency. In the studied compound there is mismatch of peaks of different temperatures which suggests short range motion of charge carrier and departure from ideal Debye-like behavior.

3.2 Complex Electric Modulus Analysis

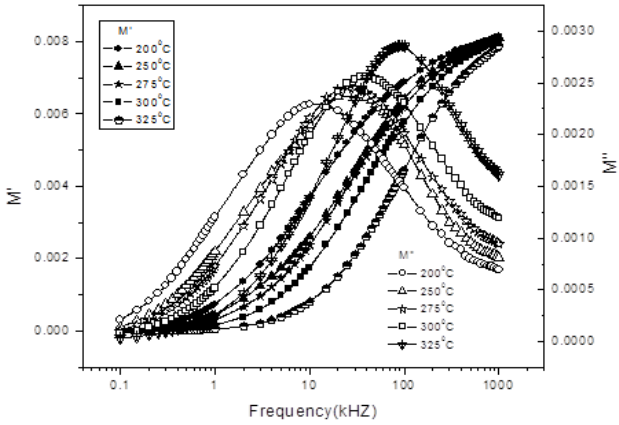

Fig.4. Variation of M' and M'' with frequency at different temperatures of NNdT.

Electrical modulus studies can be used to detect electrode polarization, grain boundary conduction effects, bulk properties, electrical conductivity, and the relaxation mechanism [20]. Fig 4. shows the variation of M′ and M″ with frequency at selected temperatures. M″ is characterized by a very low value (almost zero) in the low frequency region then a continuous increase with an increase in frequency, having a tendency to saturate at a maximum asymptotic value in the high frequency region for all temperatures. This is attributed to the presence of conduction phenomena due to short-range mobility of charge carriers [21]. Since M′ reaches a constant value for each temperature at higher frequency, the absence of an appreciable electrode polarization in the temperature domain studied is confirmed. In the frequency-temperature dependence of imaginary part of electric modulus (M″) plot, M''_{max} shifts towards higher relaxation frequencies with a rise in temperature. This behaviour suggests that dielectric relaxation is thermally activated in which the hopping mechanism of charge carriers dominates intrinsically [22]. Asymmetric broadening of the peak indicates a spread of relaxation with different time constants, and hence the relaxation in the material is of a non-Debye type.

3.3 J-E characteristics

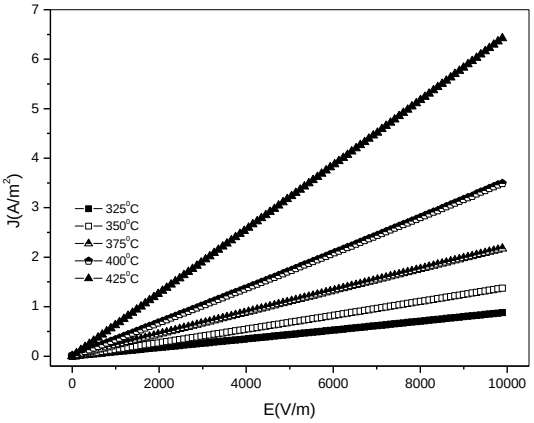

Fig.5. Variation of current density with applied electric field at different temperatures of NNdT..

Fig. 5. shows the variation of current density (J) with applied field (E) at different temperatures in the sample. The current density increases with rise in temperature in the sample showing the NTCR behavior of the material. As the nature of variation of current density with applied field at a particular temperature deviates from Ohm's law, it indicates the semiconducting nature of the material.

3.4 AC Conductivity

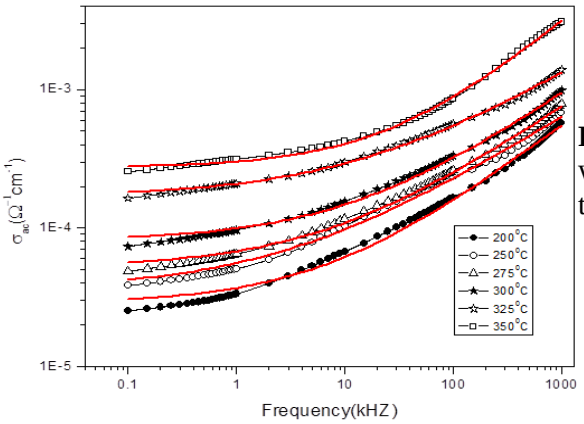

Fig.6. Variation of ac conductivity with frequency at different temperatures of NNdT.

The frequency dependence of ac conductivity, σ(ω), at various temperature is shown in Fig. 6. At low temperatures the conductivity increases with rise in frequency, which is a characteristic of ω^n (n=exponential). At high temperatures and low frequencies conductivity shows a flat response while it has ω^n

dependence at high frequencies. The phenomenon of the conductivity dispersion in solids is generally analyzed using Jonscher's power law; [23] $\sigma_{ac} = \sigma_{dc} + A\omega^n$, where σ_{dc} is the dc conductivity (frequency independent plateau in the low frequency region), A is the temperature dependent frequency pre-exponential factor and n is the power law exponent in the range of $0 \leq n \leq 1$. The exponent n represents the degree of interaction between mobile ions with the lattice around them, and the pre exponential factor A determines the strength of polarizability. The material obeys the universal power law, and is confirmed by a typical fit of the above equation to the experimental data at various temperatures.In the high frequency region the curves approach to each other. The nature of conductivityplots reveals that the curves exhibit low frequency dispersion phenomena obeying the Jonscher's power law. Fromnon-linear fitting it is found that the motion of charge carriers inthe samples is translational one because of small value of n (<1)[24].

3.5 DC Conductivity

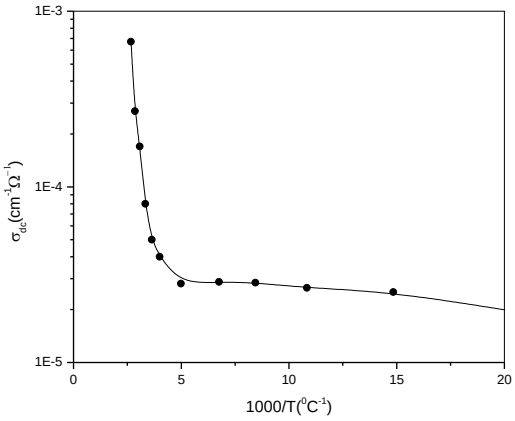

Fig.7. Variation of dc conductivity as a function of temperature of NNdT.

Fig. 7. shows the variation of dc conductivity with respect to inverse of absolute temperature. The value of bulk conductivity of the material was evaluated from the complex impedance plots of the sample at different temperatures using the relation: $\sigma_{dc} = t / R_b A$, where R_b is the bulk resistance, t the thickness and A is the surface area of the sample respectively. The dc conductivity increases with rise in temperature confirming the negative temperature co-efficient of resistance (NTCR) behavior. This plot follows the Arrhenius relation: $\sigma_{dc} = \sigma_o e^{-\frac{E_a}{K_B T}}$.

4. Conclusion

The polycrystalline sample of $Na_2Pb_2Nd_2W_2Ti_4Ta_4O_{30}$ has been prepared by a high-temperature solid-state reaction technique. Preliminary structural analysis confirmed the formation of a single phase material in an orthorhombic system at room temperature. Study of electrical behavior using complex impedance analysis (CIS) provides information on the presence of both grain and grain boundary effects in the material. Modulus analysis indicates non-exponential type of conductivity relaxation in the material. The ac conductivity obeys the universal power law and the dispersion in conductivity has been observed in the lower frequency region. The variation of dc conductivity (bulk) as a function of temperature demonstrates that the compound has Arrhenius type of electrical conductivity and NTCR behavior like semiconductor.

References

[1] A K Singh, RNP Choudhary, *Ferroelectrics*, **325**, 7 (2005)

[2] MS Kim, JH Lee, JJ Kim, HY Lee, SH Cho, *J. Solid-State Electrochem*. **10**, 18 (2006)

[3] L Fang, H Zhang, TH Huang, RZ Yuan, HX Liu, *J. Mater. Sci*. **40**, 533 (2005)

[4] R Padhee, PR Das, BN Parida, and RNP Choudhary, *J. Elec. Mat*. **42**, 426 (2013)

[5] BN Parida, PR Das, *J. All. Comp*. **585**, 234 (2014)

[6] L Biswal, PR Das, B Behera, RNP Choudhury, *J. Elec. Ceram*. **29**, 204 (2012)

[7] S Saparjya, S Behera, B Behera, PR Das, *J. Mat. Sci: Mat. Elec*. DOI 0.1007/s10854-016-5995-y

[8] S Behera, BN Parida, P Nayak and PR Das, *J. Mat. Sc, Mat. Electron* **24**, 1132 (2013)

[9] S Behera, PR Das, P Nayak , SK Patri. *J. Elect.Mat*. (2016). DOI 10.1007/s 11664-016-5061-9

[10] PR Das, S Behera, P Nayak. *AIP Conf. Proc*.**1372**, 33 (2011)

[11] JR. MacDonald, *Impedance Spectroscopy* (Wiley, New York, 496, 1987)

[12] B Yeum, ZSimpWin Version 2.00, Echem Software Ann Arbor, MI, USA

[13] KS Rao, D M Prasad, PM Krishna, JH Lee, *Physica* **B 403**, 2079 (2008)

[14] IM Hodge, MD Ingram, and AR West, *J. Electroanal. Chem*. **58**, 429 (1975)

[15] S Sen, RNP Choudhary, P Pramanik, *Phys*. **B 387**, 56 (2007)

[16] J Plocharski and W Wieczoreck, *Solid State Ionics* **28**, 979 (1988)

[17] A K Jonscher, *Nature* **267**, 673 (1977)

[18] CK Suman, K Prasad and RNP Choudhary, *J. Mater. Sci*. **41**, 369 (2006)

[19] DC Sinclair and AR West,'.*J.Appl. Phys*. **66**, 3850 (1989)

[20] JR Macdonald, *Solid State Ionics*, **13**, 147 (1984)

[21] PS Das, PK Chakraborty, B Behera, RNP Choudhary, *Phys. B* **395**, 98 (2007)

[22] P Ganguly, AK Jha, KL Deori, *Solid. State. Com*.**146**, 472 (2008)

[23] AK Jonscher, *Nature* **267**, 673 (1977)

[24] K Funke, *Solid State Chem*. **22**, 111 (1993)